RADIO SCIENCE, VOL. 42, RS2S06, doi:10.1029/2006RS003456, 2007

Relative importance of the day-night asymmetry in Schumann resonance amplitude records

O. Pechony,[1] C. Price,[1] and A. P. Nickolaenko[2]

Received 8 January 2006; revised 26 January 2007; accepted 8 February 2007; published 17 March 2007.

[1] Computations of Schumann resonance (SR) field amplitudes from a point source in the uniform and nonuniform cavities are performed to estimate the relative importance of the day-night asymmetry in observed SR amplitudes. Additional simulations with globally distributed sources, representing diurnal and seasonal variations of global lightning activity, are performed in uniform and nonuniform cavities to evaluate the impact of the day-night asymmetry on the diurnal and seasonal amplitude variations. The results show that the effect of diurnal ionosphere changes on the first mode SR amplitudes is ~10%. Model results indicate that the source properties (the level of activity and proximity to the observer) play the dominant role in the diurnal variations observed in SR field records, with the day-night asymmetry being secondary in importance.

Citation: Pechony, O., C. Price, and A. P. Nickolaenko (2007), Relative importance of the day-night asymmetry in Schumann resonance amplitude records, *Radio Sci.*, *42*, RS2S06, doi:10.1029/2006RS003456.

1. Introduction

[2] Schumann resonances (SR), resonant electromagnetic waves in the extremely low frequency (ELF) range in the Earth-ionosphere cavity induced by lightning discharges, were predicted by *Schumann* [1952] and detected by *Balser and Wagner* [1960]. Applications for SR include evaluation of characteristics of global thunderstorm activity, monitoring changes in planetary temperature [*Williams*, 1992] and global upper tropospheric water vapor [*Price*, 2000; *Price and Asfur*, 2007], lower ionosphere studies and exploration of the electrical activity on celestial bodies [*Nickolaenko and Rabinowicz*, 1982; *Sentman*, 1990].

[3] One of the recently debated issues in SR studies is the terminator effect, treated for the first time by *Madden and Thompson* [1965] and *Bliokh et al.* [1968]. Diurnal variations of the SR field power were the first well-documented features of the SR phenomenon. The observed variations were explained by the alterations in the source-receiver geometry and it was concluded that no particular systematic changes of the ionosphere are needed to explain these variations [*Balser and Wagner*, 1962; *Madden and Thompson*, 1965]. Subsequent theoretical studies supported these estimates [*Bliokh et al.*, 1980; *Field and Joiner*, 1982; *Nickolaenko*, 1986; *Rabinowicz*, 1988; *Nickolaenko and Hayakawa*, 2002]. However, experimental observations showed that SR intensities recorded at different sites show a better agreement in local time (LT) rather than in universal time (UT), suggesting that SR intensities may be modulated by local effects. The technique for separating the global and the local contributions to the recorded SR power was suggested by *Sentman and Fraser* [1991], who interpreted the local contribution as the diurnal variation of the ionosphere height. *Pechony and Price* [2006] show that a similar local contribution function can be obtained when fields computed with a uniform model are analyzed, suggesting that the local contribution represents source-receiver distance variations, rather then diurnal variations of ionosphere height. The structure of the observed diurnal and seasonal variations of SR fields, enhancement of amplitudes during the daytime with significant variations around sunrise and sunset in many records, gave rise to the hypothesis that SR amplitude records are significantly influenced by ionosphere day-night asymmetry [*Sentman and Fraser*, 1991; *Melnikov et al.*, 2004]. *Sátori et al.* [2007] present records from Nagycenk (Hungary) station that demonstrate changes in SR amplitudes around ionospheric sunrise and sunset times. *Sentman and Fraser* [1991] and *Williams and Sátori* [2004] suggested that in order to use SR records as a proxy for global lightning activity, they must be corrected for the day-night asymmetry effect. However, recent theoretical results obtained by *Yang and Pasko* [2006] confirmed that power variations of the first SR mode during sunrise and sunset are much smaller

[1]Department of Geophysics and Planetary Sciences, Tel Aviv University, Tel Aviv, Israel.
[2]Usikov Institute for Radio Physics and Electronics, Ukrainian National Academy of Sciences, Kharkov, Ukraine.

0048-6604/07/2006RS003456$11.00

than those associated with variations of global lightning activity, thus global lightning activity should play a more important role in the variations of the SR power.

[4] Computer modeling allows one to separate completely different effects, ionosphere variations and global thunderstorm activity. Here we present computer simulations of diurnal-seasonal changes in SR field amplitudes for a single source, as well as for global lightning distributions, derived from 5 years of Optical Transient Detector (OTD) lightning data [*Christian et al.*, 2003]. The calculations were performed with the partially uniform knee (PUK) model which allows simulations both with and without the day-night asymmetry of the ionosphere [*Pechony and Price*, 2004].

2. Model Description

[5] Recent studies return to modeling of resonance oscillations in the frameworks of transmission line and finite difference time domain (FDTD) models [*Mushtak and Williams* 2002; *Morente et al.*, 2003; *Otsuyama et al.*, 2003; *Pechony and Price*, 2004; *Ando and Hayakawa*, 2004; *Ando et al.* 2005; *Yang and Pasko*, 2005]. The PUK model [*Pechony and Price*, 2004] used in this work is a combination of two techniques: the "knee" model developed by *Mushtak and Williams* [2002], which addresses the problem of approximating the knee-like conductivity profile (on a semilogarithmic scale) of the Earth's ionosphere, and the "global partially uniform day-night" model by *Kirillov et al.* [1997], which allows for a convenient treatment of the day-night asymmetry of the ionosphere.

[6] *Madden and Thompson* [1965] suggested using a formal analogy between ELF wave propagation within a waveguide with wave propagation in a transmission line for numerical modeling of ELF radio waves in the spherical Earth-ionosphere waveguide. This method was fully developed by *Kirillov* [1993] into the two-dimensional telegraph equation (TDTE) technique and is thoroughly described in a series of papers: *Kirillov* [1993, 1996], *Kirillov et al.* [1997], and *Kirillov and Kopeykin* [2002]. ELF wave propagation in the Earth-ionosphere cavity excited by a vertical dipole of the dipole moment P located at (θ_S, φ_S) on the Earth surface, corresponding to the point voltage source u_S, can be described in terms of TDTE by [*Kirillov et al.*, 1997]

$$\begin{aligned} &\mathrm{div}\left(\mathrm{L}^{-1}\mathbf{grad}\mathrm{u}\right) + \omega^2\mathrm{C}(\mathrm{u}+\mathrm{u_s}) = 0 \\ &\mathrm{u_s} = (\mathrm{P}/\varepsilon_0)(\delta(\theta-\theta_\mathrm{s})/\mathrm{a}^2\sin\theta) \end{aligned} \tag{1}$$

where ω is the angular frequency ($\exp(-i\omega t)$ time dependence is assumed), a is the Earth radius, $u = \int_0^\infty E_r dr$ is the voltage, $L = -\mu_0 H_M$ is the local inductance and $C = \varepsilon_0/H_E$ is the surface capacitance. H_E and H_M are the lower and the upper characteristic altitudes. Their real parts can be considered as the effective "electric" and "magnetic" ELF heights of the waveguide [*Greifinger and Greifinger*, 1978]. These parameters are frequency-dependent and incorporate the vertical distributions of ionosphere's electrodynamic properties. The lower characteristic altitude $H_E(f)$ is computed as an integral

$$\mathrm{H_E} = \int_0^\infty \frac{\mathrm{dz}}{1 + \mathrm{i}\sigma(\mathrm{z})/(2\pi\mathrm{f}\varepsilon_0)} \tag{2}$$

where σ is the conductivity.

[7] The widely used two-exponential model developed by *Greifinger and Greifinger* [1978] assumes exponential conductivity profiles within two characteristic layers responsible for the behavior of the electric and magnetic field components. The two-exponential model successfully predicts resonance frequencies but fails to provide an adequate simulation of the frequency dependence of the quality factors in the SR band, which requires taking into consideration the knee-like area in the conductivity profile (on a semilogarithmic scale), which marks a transition from ion-dominated to electron-dominated conductivity [*Galejs*, 1962; *Wait*, 1964; *Cole*, 1965; *Madden and Thompson*, 1965; *Jones*, 1967; *Jones and Knott*, 1999; *Mushtak and Williams*, 2002; *Knott and Jones*, 2003]. It is highly desirable to approximate the conductivity profile with a function, which allows for the analytical solution of the integral in equation (2). *Mushtak and Williams* [2002] successfully solved this problem by approximating the conductivity profile with two exponents, below and above the "knee" altitude:

$$\begin{aligned} \sigma(\mathrm{z}) &= \sigma_{\mathrm{kn}}\exp[(\mathrm{z}-\mathrm{h_{kn}})/\zeta_\mathrm{b}];\ \mathrm{z} < \mathrm{h_{kn}} \\ \sigma(\mathrm{z}) &= \sigma_{\mathrm{kn}}\exp[(\mathrm{z}-\mathrm{h_{kn}})/\zeta_\mathrm{a}];\ \mathrm{z} \geq \mathrm{h_{kn}} \end{aligned} \tag{3}$$

where σ_{kn} is the conductivity at a symbolically defined "knee" altitude h_{kn}, and ζ_b and ζ_a are the scale heights of the exponential functions approximating the conductivity profile below and above h_{kn}, respectively. The multiknee model developed by *Pechony and Price* [2004] further extends the applicability of the "knee" model, allowing to approximate yet more complicated conductivity profiles.

[8] Following *Mushtak and Williams* [2002], the characteristic altitudes H_E and H_M are expressed as

$$\begin{aligned} \mathrm{Re\,H_E(f)} &= \mathrm{h_{kn}} + \zeta_\mathrm{a}\ln\left(\frac{\mathrm{f}}{\mathrm{f_{kn}}}\right) + \frac{1}{2}(\zeta_\mathrm{a}-\zeta_\mathrm{b}) \\ &\quad\cdot\ln\left[1+\left(\frac{\mathrm{f_{kn}}}{\mathrm{f}}\right)^2\right] \\ \mathrm{Im\,H_E} &= -\frac{\pi}{2}\zeta_\mathrm{a} + (\zeta_\mathrm{a}-\zeta_\mathrm{b})\arctan\left(\frac{\mathrm{f_{kn}}}{\mathrm{f}}\right) \end{aligned} \tag{4}$$

$$\begin{aligned} \mathrm{Re\,H_M(f)} &= \mathrm{h_m^* - \zeta_m(f)\ln\left(f/f_m^*\right)} \\ \mathrm{Im\,H_M} &= \frac{\pi}{2}\zeta_m(\mathrm{f}) \end{aligned} \tag{5}$$

where $f_{kn} = \sigma_{kn}/(2\pi\varepsilon_0)$. The scale height ζ_m depends on frequency as $\zeta_m(f) = \zeta_m^* + b_m(1/f - 1/f_m^*)$; h_m^* and ζ_m^* are, respectively, the real part of the characteristic altitude and the "effective" scale height at an arbitrary frequency f_m^* [*Mushtak and Williams*, 2002]. The altitude $h_m^*(f)$ can be determined from equation (6) [*Kirillov*, 1993; *Mushtak and Williams*, 2002]:

$$\begin{aligned} &\left[\frac{1}{1.78}\left(\frac{1}{\zeta_{Ne}} + \frac{1}{|\zeta_\nu|}\,\frac{\nu_e^2(h_m^*)}{\nu_e^2(h_m^*) + \omega_{Hz}^2}\right)\right]^2 \\ &\quad \cong \frac{k_0\omega_0^2(h_m^*)}{2\pi f\sqrt{\nu_e^2(h_m^*) + \omega_{Hz}^2}} \end{aligned} \tag{6}$$

where k_0 is the free space wave number, ω_0 is the electron plasma frequency, ω_{Hz} is the vertical projection of the electron gyrofrequency, ν_e is the electron collision frequency, ζ_{Ne} and ζ_ν are the scale heights of the exponential approximations of the electron density and electron collision frequency profiles, respectively.

[9] The electromagnetic field components are calculated as $\varepsilon_0 E_r = Cu$, $H_\varphi = -j_\theta$ and $H_\theta = j_\varphi$ at the Earth's surface [*Kirillov*, 1993]. The surface current density j is calculated from $i\omega L\boldsymbol{j} = \boldsymbol{grad}u$ [*Kirillov*, 1993]. The voltage $u(\theta, \varphi)$ originating from a vertical dipole source can be described by equation (7) [*Kirillov et al.*, 1997]:

$$\begin{aligned} u(\theta,\varphi) &= \frac{k^2S^2P}{2\pi\varepsilon_0}\sum_{m=0}^{\infty}\varepsilon_m u_m(\theta)\cos[m(\varphi-\varphi_S)], \\ \varepsilon_m &= \begin{cases} 1 \text{ for } m = 0 \\ 2 \text{ for } m > 0 \end{cases} \end{aligned} \tag{7}$$

where S is the complex sine of the wave incidence angle (see below). In terms of the "global partially uniform" day-night model [*Kirillov et al.*, 1997] the waveguide parameters are approximated by their average values for the day and for the night. In this manner the waveguide is divided into two hemispheres, day and night, each uniform (hence "partially uniform" model). The problem is formulated in a spherical coordinate system (r, θ, φ) centered at nadir with a steep terminator (instantaneous transition from daytime to nighttime ionospheric condition) located at 81° from nadir [*Kirillov et al.*, 1997]. For a dayside source the solution is derived starting with a uniform sphere with daytime parameters and then reflection and transmission at the day-night boundary are accounted for. Similar procedure is repeated for a nightside source. For a uniform sphere with dayside parameters [*Kirillov et al.*, 1997],

$$u_m(\theta) = c_m\begin{cases} P^m_{\nu_{day}}(-\cos\theta_S)P^m_{\nu_{day}}(\cos\theta), \theta < \theta_S \\ P^m_{\nu_{day}}(\cos\theta_S)P^m_{\nu_{day}}(-\cos\theta), \theta > \theta_S \end{cases} \tag{8}$$

where the c_m satisfies equation (9):

$$\begin{aligned} c_m \sin\theta_S\Big[&P^m_{\nu_{day}}(\cos\theta_S)\frac{d}{d\theta_S}P^m_{\nu_{day}}(-\cos\theta_S) \\ &-P^m_{\nu_{day}}(-\cos\theta_S)\frac{d}{d\theta_S}P^m_{\nu_{day}}(\cos\theta_S)\Big] = -1 \end{aligned} \tag{9}$$

Taking into account the reflection from and transmission through the terminator, we have

$$\begin{aligned} u_m^{night}(\theta) &= D_m c_m P^m_{\nu_{day}}(-\cos\theta_S)P^m_{\nu_{night}}(\cos\theta) \\ u_m^{day}(\theta) &= u_m(\theta) + R_m c_m P^m_{\nu_{day}}(-\cos\theta_S)P^m_{\nu_{day}}(-\cos\theta) \end{aligned} \tag{10}$$

Reflection and transmission coefficients R_m and D_m are computed by using the continuity condition for the voltage (the analog of the electric field in a transmission line) and for the normal component of the current (the analog of the magnetic field) formulated at the day-night boundary. The coefficients are expressed by [*Kirillov et al.*, 1997]
where θ_T defines the boundary between day and night

$$\begin{aligned} -R_m &= \frac{L_{night}^{-1}P^m_{\nu_{day}}(\cos\theta_T)\frac{d}{d\theta_T}P^m_{\nu_{night}}(\cos\theta_T) - L_{day}^{-1}P^m_{\nu_{night}}(\cos\theta_T)\frac{d}{d\theta_T}P^m_{\nu_{day}}(\cos\theta_T)}{L_{night}^{-1}P^m_{\nu_{day}}(-\cos\theta_T)\frac{d}{d\theta_T}P^m_{\nu_{night}}(\cos\theta_T) - L_{day}^{-1}P^m_{\nu_{night}}(\cos\theta_T)\frac{d}{d\theta_T}P^m_{\nu_{day}}(-\cos\theta_T)} \\ D_m &= \frac{L_{day}^{-1}P^m_{\nu_{day}}(-\cos\theta_T)\frac{d}{d\theta_T}P^m_{\nu_{day}}(\cos\theta_T) - L_{night}^{-1}P^m_{\nu_{day}}(\cos\theta_T)\frac{d}{d\theta_T}P^m_{\nu_{day}}(-\cos\theta_T)}{L_{night}^{-1}P^m_{\nu_{day}}(-\cos\theta_T)\frac{d}{d\theta_T}P^m_{\nu_{night}}(\cos\theta_T) - L_{day}^{-1}P^m_{\nu_{night}}(\cos\theta_T)\frac{d}{d\theta_T}P^m_{\nu_{day}}(-\cos\theta_T)} \end{aligned} \tag{11}$$

Table 1. Model Input Variables for the Uniform and the Day-Night Models

	f_{kn}, Hz	h_{kn}, km	ζ_b, km	ζ_a, km	f_m^*, Hz	h_m^*, km	ζ_m^*, km	b_m, km
Uniform	13.0	57.0	8.3	3.25	6.0	98.3	3.6	4.5
Day	13.0	54.0	7.5	2.7	6.0	97.5	3.7	5.0
Night	13.0	60.0	9.1	3.8	6.0	99.0	3.5	4.0

hemispheres, the terminator. The Legendre functions are calculated by using the convergence acceleration method by *Nickolaenko and Rabinowicz* [1974] (corrected formulas can be found in work by *Connor and Mackay* [1978], *Bliokh et al.* [1980], and *Nickolaenko and Hayakawa*, [2002]). The complex parameter ν is calculated via the relationship $\nu(\nu + 1) = S^2 k_0^2 a^2$, and the complex sine $S^2 = H_M(f)/H_E(f)$ [*Kirillov*, 1993].

[10] The resulting model can be operated in either uniform or day-night mode. The model input variables for both uniform and day-night models are summarized in Table 1. Specific values for the model input variables were selected following *Pechony and Price* [2004]. Variables for the lower characteristic altitude were modified to achieve a better agreement with the *Cole and Pierce* [1965] conductivity profile (including the difference between the day and night conductivity profiles). Computed propagation parameters, the phase velocity $V_{ph}(f) = c/\mathrm{Re}S(f)$ (where c is the speed of light) and the attenuation rate $\alpha(f) = 0.182|\mathrm{Im}S(f)|$ [dB/Mm], are shown in Table 2 and are compared to the values published by *Galejs* [1972], showing a close agreement with the previously published results. *Greifinger et al.* [2005] estimated experimentally that the night/day ratio of lower characteristic altitudes ranges from 1.1 to 1.24, with the mean value at 1.19, for the 5–17 Hz frequency range covering the first and second SR modes. The first mode alone should yield lower night/day ratio. The PUK model shows ~1.12 night/day ratio (55 and 49 km) for the first mode, which is in accordance with these results. The following calculations are performed at the first mode resonant frequency, 7.8 Hz.

[11] All the simulations are performed with hourly time resolution. This is sufficient to study the rate of influence of day/night ionosphere conditions on SR amplitude records by comparing the mean daytime and nighttime amplitudes in a day/night cavity excited by a single source and by comparing amplitudes simulated in uniform and day/night models. If one is interested in utilizing this model for fine time resolution simulations, a gradual terminator must be taken into account.

3. Single-Source Simulations

[12] In the single-source simulations only one stationary (constant location) source excites the cavity throughout the day. Therefore the field alterations present in these simulations are caused only by the ionosphere variations. The purpose of the computations is to test the influence of the day-night asymmetry itself, in the absence of the source motion.

[13] Figure 1 illustrates the distortion of the electric field (first mode, 7.8 Hz) by the day-night terminator, in a cavity exited by a single source, as calculated with the PUK model. The source is located in Africa (5°S, 25°E). The terminator is shown by a dashed line and the source location is marked by a cross. As expected, the magnitude of the electric field increases on the dayside.

[14] Figure 2 shows the diurnal variation of the first SR mode electric field amplitude calculated in the day-night and uniform cavities for a receiver located in Mitzpe Ramon, Israel (32°N, 34°E), and the same source located in Africa (5°S, 25°E). Figure 2 shows clear diurnal variations of the field amplitude calculated with the day-night model. Note that the field is not only a function of the ionosphere properties (day or night) above the source and the receiver, but also depends on their proximity to the terminator line which serves as a reflection/transmission boundary [*Nickolaenko*, 1986; *Rabinowicz*, 1988; *Nickolaenko and Hayakawa*, 2002]. Naturally, the uniform model results in no diurnal field variations for a source with constant location and intensity. The mean daytime and mean nighttime amplitude levels were calculated between the sunrise and sunset at the receiver, excluding the sunrise and sunset hours (as they do not fully refer either to day or to night). The disturbance introduced by the day-night asymmetry results in around ±6% deviation from the amplitudes obtained in the uniform cavity (see Figure 2), or a 12% difference between the mean daytime and nighttime values. This value increases to ±11% for the second mode and further increases with increasing frequency. This is in agreement with *Melnikov et al.* [2004], *Greifinger et al.* [2005], and *Sátori et al.* [2007], who demonstrate that the effect of the day-night asymmetry increases with frequency.

Table 2. Comparison of Propagation Parameters at $f = 10$ Hz for *Galejs* [1972] and PUK Day-Night Model

	c/V_{ph} (day)	c/V_{ph} (night)	$\alpha_{(\mathrm{day})}$	$\alpha_{(\mathrm{night})}$
Galejs [1972]	1.36	1.32	0.2	0.3
PUK	1.35	1.29	0.2	0.3

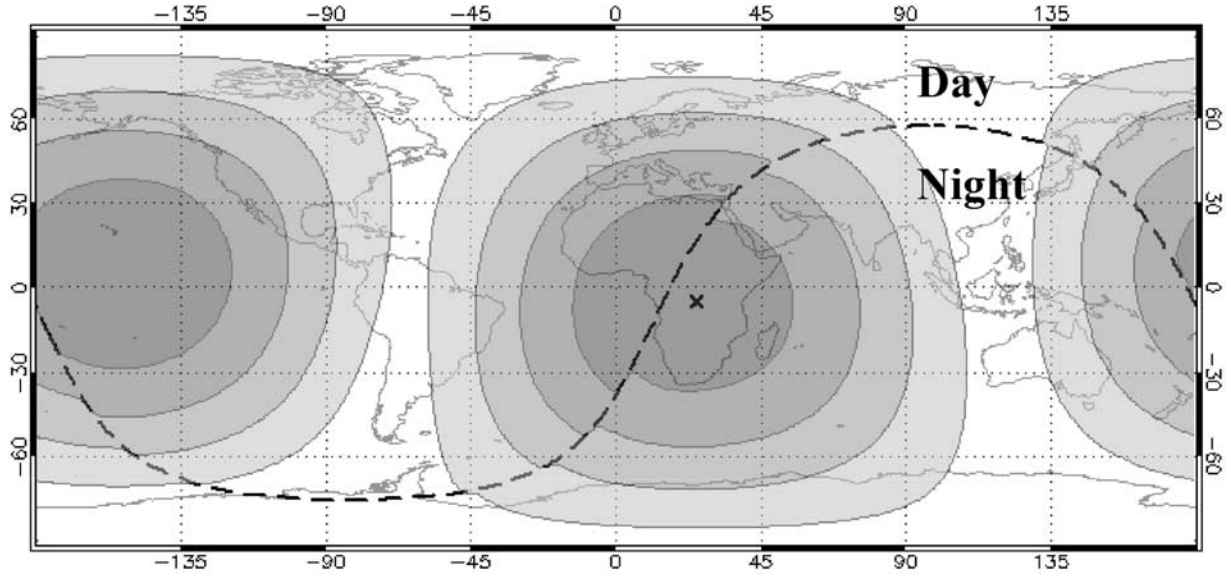

Figure 1. Distortion of the electric field by the day/night terminator (dashed line). The source location (5°S, 25°E) is marked by a cross.

[15] In order to check the sensitivity of the day-night cavity simulation results to the selected ionosphere profile, the first mode amplitudes were recalculated for an alternative conductivity profile, suggested by V. C. Mushtak (personal communication, 2006). The daytime profile parameters are as follows: h_{kn} = 49 km; f_{kn} = 1.1 Hz; ζ_b = 10.7 km; ζ_a = 2.4 km. The nighttime profile parameters are h_{kn} = 63 km; f_{kn} = 3.6 Hz; ζ_b = 10.7 km; ζ_a = 2.4 km. Figure 3 shows the resulting profile together with the conductivity profile from *Cole and Pierce* [1965], and the fitted profile used for simulations is this work. The alternative profile notably differs from the profile used for simulations in this work and results in

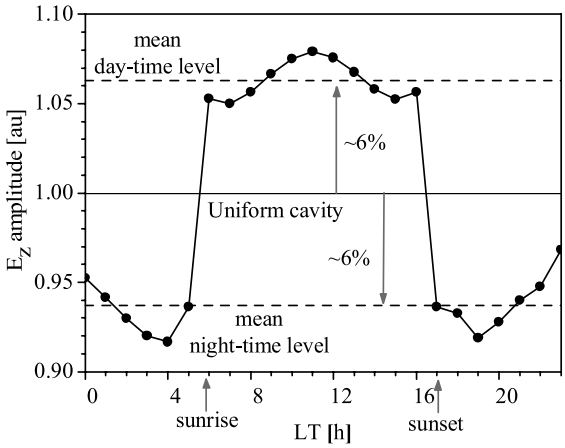

Figure 2. PUK calculated electric field amplitudes for day-night and uniform models for a receiver located in Mitzpe Ramon (32°N, 34°E) from a single stationary source in Africa (5°S, 25°E). The dashed horizontal lines indicate the mean daytime (top line) and mean nighttime (bottom line) amplitude levels.

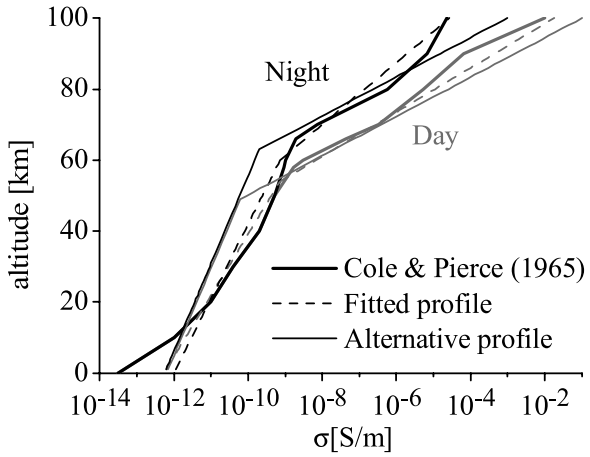

Figure 3. Conductivity profiles: profile adopted from *Cole and Pierce* [1965] (thick solid line); fitted profile, used for simulations in this work (dotted lines); and alternative profile suggested by V. C. Mushtak (personal communication, 2006) (thin solid lines).

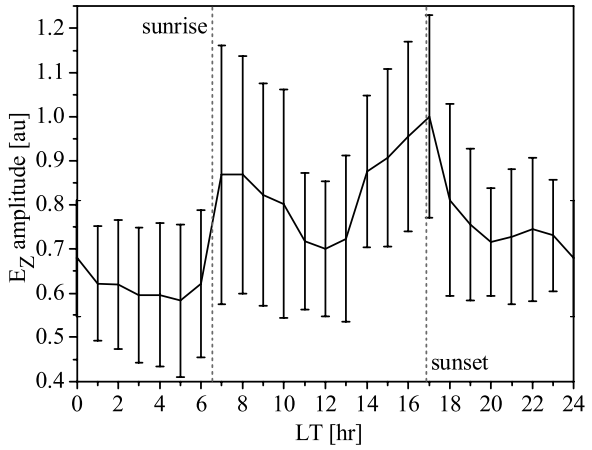

Figure 4. Experimental electric field amplitudes (first mode) collected at Mitzpe Ramon in January 2000. Solid line shows monthly mean value. Error bars indicate standard deviation.

higher (1.19) night/day ratio of lower characteristic altitudes. Nevertheless the effect of the day-night asymmetry, calculated with this profile, is still very low, about ±8%.

[16] The small effect of the day-night asymmetry may be explained by the large size of the first Fresnel zone. In WKB (Wentzel-Kramers-Brillouin) approximation the size of the first Fresnel zone provides an estimate for the disturbance effect [*Field and Joiner*, 1982]. As the size of the first Fresnel zone increases, the disturbance effect weakens. The size of the Fresnel zone is determined by the source-receiver distance and the wave frequency, increasing with increasing source-receiver distance and with decreasing frequency [*Barclay*, 2003]. It can be shown that at the first SR mode the first Fresnel zone covers as much as 66% of the Earth surface for the closest major source, Africa (source-receiver distance ~5 Mm). For an American source (source-receiver distance ~10 Mm) the first Fresnel zone coverage reaches 100% at the first SR mode. For the third mode the first Fresnel zone is still considerably large compared to the size of the disturbed portion of the waveguide. For higher frequencies the size of the first Fresnel zone decreases, concentrating around the great circle connecting the source and the receiver, and the contribution of the day-night asymmetry becomes more pronounced.

[17] Model results indicate that the terminator effect plays a significant role when fields arrive from a single source along the fixed path, such as ELF transients. The calculated ionosphere-induced disturbance (±6% deviation or 12% change, for the first SR mode) is less than both diurnal and day-to-day SR signal variations. Figure 4 shows January 2000 monthly mean SR diurnal amplitude variations measured in Mitzpe Ramon (MR) site. The solid line shows the monthly mean value, and the error bars show the standard deviations (SD) of the daily records from the monthly mean value. The diurnal variation of the monthly mean SR amplitude is ~40% and often exceeds 70% on individual days. This is ~3–6 times higher then the ionosphere-induced variation. Standard deviations at a given hour range from ±12% to ±30% throughout the day with mean SD ±20% (or 40% change). Other months yield comparable and even higher SD values, reflecting severe day-to-day variability of SR records. Similar SDs were found by *Nickolaenko et al.* [1996], where records from Tottori observatory were analyzed. High day-to-day variability of SR amplitude records was also noted earlier by *Balser and Wagner* [1962]. High SD values, 2–5 times larger then the terminator effect, mean that amplitude variations caused by the day-night asymmetry at the first SR modes are buried within the "noise" level of the random natural radio signal and therefore cannot be easily segregated from experimental records.

[18] We can conclude from the above, that the ionosphere-induced variations of SR amplitudes are much smaller then the variations resulting from lightning activity. This is in accord with the recent study by *Yang and Pasko* [2006]. Using the FDTD day-night model *Yang and Pasko* [2006] found that variations in SR power related to the day-night transition are much smaller then those associated with the peaks of the global lightning activity, and therefore the global lightning activity plays a more important role in the variation of the SR power.

4. Simulations With Global Lightning Distribution

[19] The purpose of these simulations is to compare diurnal amplitude variations in uniform and nonuniform cavities resulting from the same dynamic source distribution. As a proxy for global lightning activity we use OTD data collected during a 5-year observation period.

[20] OTD lightning data are available from April 1995 through March 2000. The OTD is a space-based optical sensor on an orbit inclined by 70° with respect to the equator. The satellite orbits the Earth once every 100 min and has a 100° field of view (equivalent to ~1300 × 1300 km^2 area on the ground) [*Christian et al.*, 2003]. The OTD detects lightning flashes during both daytime and nighttime conditions with a detection efficiency ranging from 40% to 65%, depending upon external conditions. Further information can be found at the official Web site, http://thunder.nsstc.nasa.gov/otd/. OTD data are available at no charge at http://ghrc.msfc.nasa.gov/. To provide diurnal and seasonal variations of global lightning activity, OTD orbital data was recalcu-

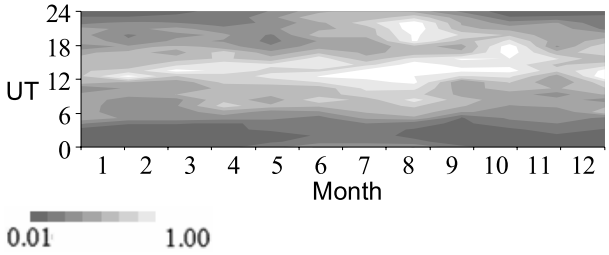

Figure 5. Diurnal-seasonal variation of diurnal monthly mean lightning activity, derived from OTD records, years 1995–2000.

lated to monthly mean diurnal data with hourly time resolution. Data for a given hour were averaged for all the days of a given month, for the 5 years. In this way 24 lightning distribution maps (one for each hour) were obtained for each month, providing diurnal monthly mean (DMM) data used as a model input. The diurnal-seasonal variation of lightning activity calculated from DMM data is presented in Figure 5, showing a peak in lightning activity around 1400 UT (African contribution), and two lower peaks around 0800 UT (Southeast Asia) and around 2000 UT (South America), with a clear enhancement of lightning activity during the northern hemisphere summer months, in consistency with the classical *Whipple* [1929] analysis.

[21] Figure 6 shows the annual mean electric field recorded at Mitzpe Ramon station (32°N, 34°E) during the years 1999–2002 (see *Melnikov et al.* [2004] for more details), together with the PUK model simulation for this station calculated from OTD DMM data (1995–2000 mean). Results are presented for both uniform (no difference between day and night ionospheric conductivity profiles) and day-night (changes in lower ionospheric profile between day and night are accounted for) models. It can be seen that both models give similar diurnal variations. The mean difference between the day-night and the uniform models does not exceed 10%, which is close to other theoretical estimates by *Nickolaenko* [1986], *Rabinowicz* [1988], and *Nickolaenko and Hayakawa* [2002] and to estimates made by *Sátori et al.* [2007] basing on experimental records. It should be noted that only a qualitative reciprocity between the model and the experiment should be expected. OTD records provide only a fraction of lightning occurring worldwide, giving a qualitative representation of global thunderstorm activity. A substantial part of global lightning activity is omitted by OTD and hence is absent in the model simulations. This activity is present as the "background" in the SR records (the characteristics of the background were studied by *Yatsevich et al.* [2005]) and hence the minimum-maximum difference in the experimental records is significantly smaller then the minimum-maximum difference in the model simulations that base on OTD data (this was also noted by *Hayakawa and Nickolaenko* [2005] and *Nickolaenko et al.* [2006]).

[22] Both experimental and modeled data show a greater contribution from Asia than from South America. This contradicts optical satellite and climatological lightning data that show the South American thunderstorm center stronger than the Asian center [*Christian et al.*, 2003]. However, note that the uniform model shows the same Asia-America ranking as the nonuniform one. This suggests that though the day-night asymmetry can enhance the 0800 UT peak, it is not responsible for the observed relative strength of the 0800 UT and 2000 UT peaks. This suggestion is supported by the experimental data presented by *Sátori et al.* [2007] for Nagycenk, Hungary station where both the original record and the record "corrected" for the day-night asymmetry show 0800 UT peak stronger than 2000 UT peak. Asian and American thunderstorms are not the only SR sources at the corresponding 0800 UT and 2000 UT. While the two thunderstorm centers dominate the global lightning activity at these hours, there is still substantial lightning activity in other regions at these times. The relative strength of the 0800 UT and 2000 UT peaks in SR records is influenced by the global lightning activity, and while the Asian thunderstorm center may be weaker then the American, the distribution of the global lightning activity can result in a higher SR record at 0800 UT than at 2000 UT at the MR station. Furthermore, the nodal structure of the SR fields, i.e., the source-receiver distance influence, can also result in such "invert ranking". The difference in the source-receiver distances of the Asian and American sources from Israel result in

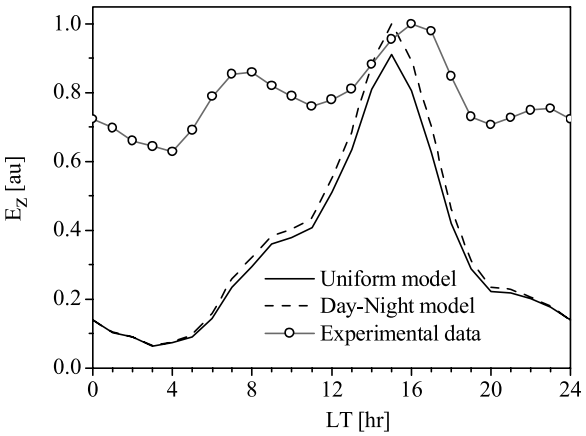

Figure 6. Annual mean electric field at Mitzpe Ramon station: simulation results for 1995–2000 OTD DMM lightning distribution (uniform and day-night modes) and experimental data (1999–2002 mean).

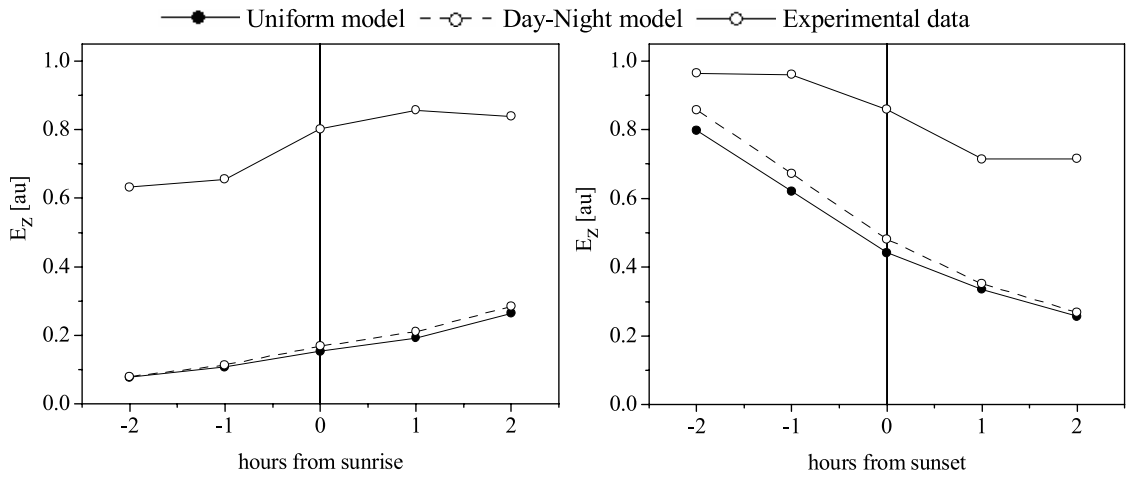

Figure 7. Annual mean electric field at Mitzpe Ramon station at sunrise and sunset: simulation results for 1995–2000 OTD DMM lightning distribution (uniform and day-night modes) and experimental data (1999–2002 mean).

weaker amplitudes from the South American sources then from the Asian sources. A source located in Asia can produce ~10% higher amplitudes (depending on the exact source location) at Mitzpe Ramon then the same source located in South America.

[23] Figure 7 shows the mean annual variation of the electric field amplitude during sunrise and sunset. The plot was built accounting for the variation of sunrise and sunset times throughout the year. Mitzpe Ramon field records and PUK model simulations (both uniform and day-night) are shown. The general trend of the field variations is equally well simulated by the uniform and day-night models; however, inclusion of the day-night asymmetry sharpens the changes at sunrise and sunset.

[24] The general SR field pattern is rather well simulated by both uniform and day-night models. The contribution of the terminator effect does not exceed 10% for the first SR mode. However, this is likely to be an overestimated value since a steep terminator is assumed in the model (i.e., the change from day to night conditions is instantaneous). The real transition from day to night is gradual, which further reduces the terminator effect [*Nickolaenko*, 1986]. Resolving such small variations caused by the day-night interface from those originating from the thunderstorm motion or intensity variation is very difficult.

5. Possible Mechanism of the Observed Field Variations

[25] Below we use model simulations, and comparison with field measurements and conventional concepts of lightning climatology to present a possible mechanism that shapes the lens-like pattern in amplitude variations presented on a diurnal-seasonal scale [*Melnikov et al.*, 2004].

[26] To check the origin of the lens-like pattern, two experimental input models were used, taking to an extreme the well-known features of global lightning activity. The "follow the Sun" (FS) model exploits the fact that tropical thunderstorms develop predominantly in the afternoon: in this model there is only a single point source that moves following the sun with a 3 hr delay. FS is the simplest source model used in the SR computations [*Bliokh et al.*, 1980; *Nickolaenko and Hayakawa*, 2002] and is an extreme variation of the hot spot model introduced by *Nickolaenko et al.* [2006]. The "follow the Sun over the continents" (FSOC) model "corrects" the FS model; here the same source is activated only over the continents, since lightning activity is known to be concentrated over the land. All simulations presented below were performed in a uniform model; that is, the ionosphere nonuniformity was not taken into account.

[27] Figure 8 shows simulations with FS, FSOC and OTD DMM inputs for the Mitzpe Ramon station. The diurnal-seasonal variations of SR amplitudes computed with the FS model (Figure 8a) have a lens-shaped structure which is created as the FS source moves relative to the station, following the sun. Aside from this lens-shaped maximum, the FS model produces another, weaker, maximum around the local midnight. This is the signal from sources at the station antipode, where it is afternoon at this time.

[28] The FSOC (Figure 8b) model "turns off" the lightning of the FS model, whenever it occurs over water. For most stations, including Mitzpe Ramon, this completely wipes off the midnight maximum, since the

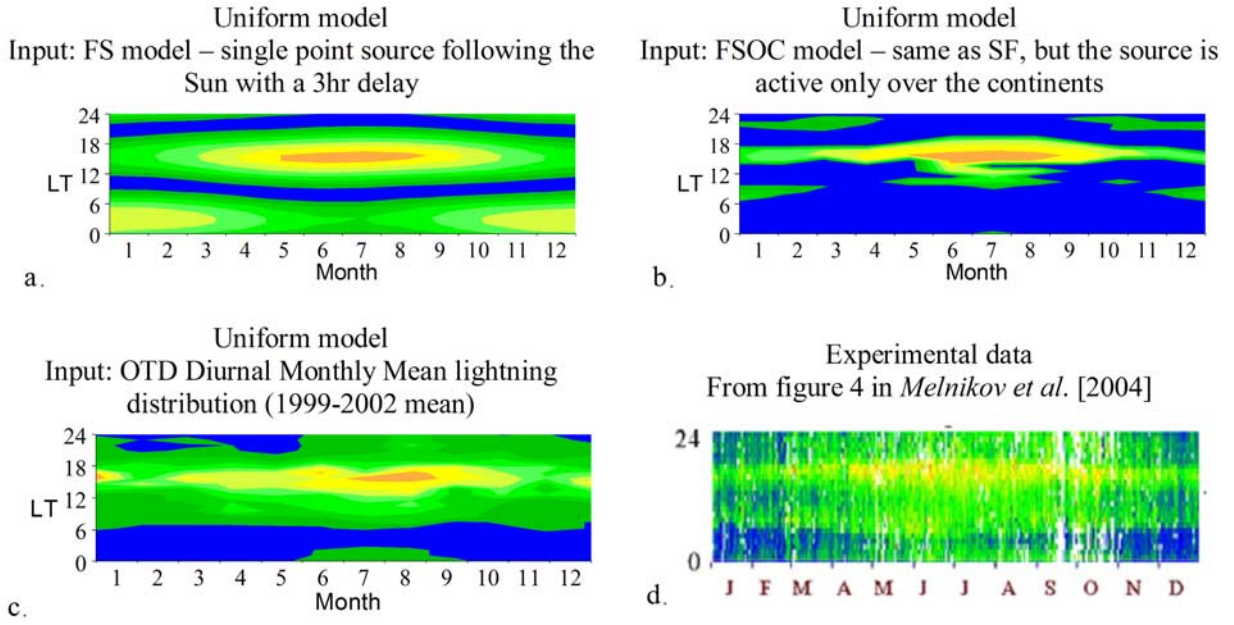

Figure 8. Diurnal-seasonal variations of the electric field amplitude at Mitzpe Ramon station resulting from FS and FSOC models, OTD DMM lightning distribution (1995–2000 mean) model, and 1999–2002 mean experimental record from *Melnikov et al.* [2004].

station antipode is located in the ocean where there is low lightning activity. Part of the dayside sources are "turned off" as well, as they fall into the seas. In the reality, thunderstorms are not strictly bounded to the continental outlines: lightning activity in the Mediterranean and over the Gulf Stream, for example, extends beyond the land and "reactivates" part of the day sources turned off by FSOC simulations. Moreover, lightning activity is strongest at local afternoon, but it does not necessarily cease during the rest of the day, adding sources not accounted for in the FS and FSOC models. Hence a wider, but more diffuse lens structure is formed for a global lightning distribution, represented by the OTD DMM lightning data used for simulations shown in Figure 8c, which reproduces the experimental data rather well (Figure 8d). Note the pronounced asymmetry that is formed in the FSOC model (Figure 8b) between the amplitudes recorded at local MR morning and evening: the evening amplitude records are much higher. This asymmetry is preserved in amplitudes calculated from global lightning distribution (Figure 8c) and is evident in the experimental records (Figure 8d; see also Figure 4 of *Melnikov et al.* [2004] for the original color plot). The asymmetry in the SR amplitudes recorded at the local morning and evening is often attributed to the local meteorological asymmetry between the dawn and dusk thunderstorms [e.g., *Sátori et al.*, 2007]. However, the local dawn-dusk meteorological asymmetry is a property of local thunderstorms, while SR records reflect the global lighting activity, and there is always dawn and dusk somewhere on the globe. The behavior of local thunderstorm around local sunrise and sunset cannot and should not directly explain the global SR records. It is only a component that, together with the seasonal thunderstorm drift and the land-ocean distribution, creates the global lightning activity characteristics which, in turn, modified by the nodal structure of the SR fields, define the characteristics of SR records.

[29] The FS and FSOC models help to separate the contribution of different factors to the variations observed in SR records. It appears that the lens-shaped structure of the field variations is crafted primarily by the movement of the sun. As the sun position changes through the day and through the year, and as thunderstorms move relative to the station, the strength of the received signal is altered. The same is true for the antipode of the station. Peculiarly, most "antipode signals" are weak since their sources are located in the ocean. The distribution of the landmasses, over which the lightning activity is concentrated, further shapes the outline of the SR records. Consequently, the lens-like pattern in the diurnal-seasonal variations in the SR field amplitudes is crafted by thunderstorm migration, driven by the sun motion and landmass distribution. This

pattern is enhanced by the additional, much weaker lens-like outline created by the ionospheric day-night asymmetry, the "terminator effect."

6. Discussion and Conclusions

[30] According to model calculations both terminator effect and diurnal-seasonal drift of global thunderstorm activity contribute to variations in SR field amplitudes. The disturbance introduced by the day-night asymmetry causes ±6% deviation from the amplitudes obtained in the uniform cavity for the first SR mode. This disturbance is less than the day-to-day SR signal variations of ±20% caused by the high variability of lightning activity and over 40% diurnal variations. The exact value of the deviations caused by the day-night asymmetry may vary with the selection of model variables; however any realistic estimate would lead to much smaller variations from the terminator effect compared to those associated with global thunderstorm activity. Therefore it appears that the general behavior of SR amplitudes is governed mostly by the variations in global lightning activity. The latter is driven by the sun movement and land-ocean distribution. The small effect of the day-night asymmetry may be explained by the large size of the first Fresnel zone which diminishes the resolution between the day and night hemispheres. The difference between the nonuniform and uniform models predicted by the PUK model is likely to be an overestimated value, since a steep terminator (instantaneous transition from light to darkness) is assumed in the computations. Real transition from day to night is about 1 Mm wide [*Kirillov et al.*, 1997], which further reduces the terminator effect [*Nickolaenko*, 1986]. Resolving such small variations caused by the day-night interface from those originating from the thunderstorm proximity or intensity variation is very difficult.

[31] Model computations indicate that information on the ionosphere can be extracted from the SR data only if the lightning distribution is carefully and correctly accounted for in the data processing. Otherwise, SR record variations provide a measure of the source proximity [*Pechony and Price*, 2006].

[32] The obtained results show, in agreement with earlier theoretical estimates [*Madden and Thompson*, 1965; *Bliokh et al.*, 1980; *Field and Joiner*, 1982; *Nickolaenko*, 1986; *Rabinowicz*, 1986, 1988; *Nickolaenko and Hayakawa*, 2002; *Melnikov et al.*, 2002] and recent work by *Yang and Pasko* [2006], that the general structure of the observed SR field variations is governed primarily by the variations in the level of lightning activity and the source-receiver geometry, and the effect of the day-night asymmetry in the ionosphere is secondary.

[33] **Acknowledgments.** We would like to thank E. R. Williams and V. C. Mushtak for the constructive criticism of the paper.

References

Ando, Y., and M. Hayakawa (2004), 2-D finite difference analyses of Schumann resonance and identification of lightning distribution, *Inst. Electr. Eng. Jpn. Trans. Fundam. Mater.*, *124*(12), 1225–1231.

Ando, Y., M. Hayakawa, A. V. Shvets, and A. P. Nickolaenko (2005), Finite difference analyses of Schumann resonance and reconstruction of lightning distribution, *Radio Sci.*, *40*, RS2002, doi:10.1029/2004RS003153.

Balser, M., and C. A. Wagner (1960), Observations of Earth-ionosphere cavity resonances, *Nature*, *188*, 638–641.

Balser, M., and C. A. Wagner (1962), Diurnal power variations of the earth-ionosphere cavity modes and their relationship to worldwide thunderstorm activity, *J. Geophys. Res.*, *67*, 619–625.

Barclay, L. (2003), *Propagation of Radiowawes*, 2nd ed., Inst. of Electr. Eng., London.

Bliokh, P. V., A. P. Nickolaenko, and Y. F. Filippov (1968), Diurnal variations of the eigen-frequencies of the Earth-ionosphere cavity in connection with the eccentricity of the geomagnetic field, *Geomagn. Aeron.*, *8*(2), 250–260.

Bliokh, P. V., A. P. Nickolaenko, and Y. F. Filippov (1980), *Schumann Resonances in the Earth-Ionosphere Cavity*, *IEE Electromagn. Ser.*, vol. 8, edited by D. L. Jones, Peter Peregrinus, London.

Christian, H. J., et al. (2003), Global frequency and distribution of lightning as observed from space by the Optical Transient Detector, *J. Geophys. Res.*, *108*(D1), 4005, doi:10.1029/2002JD002347.

Cole, R. K., Jr. (1965), The Schumann resonances, *J. Res. Natl. Bur. Stand. U.S., Sect. D*, *69*, 1345–1349.

Cole, R. K., Jr., and E. T. Pierce (1965), Electrification in the Earth's atmosphere for altitude between 0 and 100 km, *J. Geophys. Res.*, *70*, 2735–2749.

Connor, J. N. L., and D. C. Mackay (1978), Accelerating the convergence of the zonal harmonic series representation in the Schumann resonance problem, *J. Atmos. Terr. Phys.*, *40*, 977–980.

Field, E. C., and R. G. Joiner (1982), Effects of the lateral ionosphere gradients on ELF propagation, *Radio Sci.*, *17*, 693–710.

Galejs, J. (1962), A further note on terrestrial extremely low frequency propagation in the presence of an isotropic ionosphere with an exponential conductivity-height profile, *J. Geophys. Res.*, *67*, 2715–2728.

Galejs, J. (1972), *Terrestrial Propagation of Long Electromagnetic Waves*, Elsevier, New York.

Greifinger, C., and P. Greifinger (1978), Approximate method for determining ELF eigenvalues in the Earth-ionosphere waveguide, *Radio Sci.*, *13*, 831–837.

Greifinger, P., V. Mushtak, and E. Williams (2005), The lower characteristic ELF altitude of the Earth-ionosphere waveguide: Schumann resonance observations and aeronomical estimates, in *VI International Symposium on Electromagnetic Compatibility and Electromagnetic Ecology, June 21–24, 2005, Saint-Petersburg*, pp. 250–254, IEEE Press, Piscataway, N. J.

Hayakawa, S., and A. P. Nickolaenko (2005), Diurnal variations of electric activity of global thunderstorms deduced from OTD data, *J. Atmos. Electr.*, *25*(2), 55–68.

Jones, D. L. (1967), Schumann resonances and ELF propagation for inhomogeneous, isotropic ionosphere profiles, *J. Atmos. Terr. Phys.*, *29*, 1037–1044.

Jones, D. L., and M. Knott (1999), Comparison of simplified and full-wave ELF propagation models, paper presented at XXVI General Assembly, Union Radio Sci. Int., Toronto.

Kirillov, V. V. (1993), Parameters of the Earth-ionosphere waveguide at ELF, *Probl. Diffr. Wave Propag.*, *25*, 35–52.

Kirillov, V. V. (1996), Two-dimensional theory of electromagnetic wave propagation in the ELF range in the Earth-ionosphere waveguide, *Izv. Vyssh. Uchebn. Zaved Radiophyz.*, *39*, 1103–1112.

Kirillov, V. V., and V. N. Kopeykin (2002), Solving a two-dimensional telegraph equation with anisotropic parameters, *Izv. Vyssh. Uchebn. Zaved Radiophyz.*, *45*, 1011–1024.

Kirillov, V. V., V. N. Kopeykin, and V. K. Mushtak (1997), Electromagnetic waves in ELF range in the Earth-ionosphere waveguide, *Geomagn. Aeron.*, *37*(3), 114–120.

Knott, M., and D. L. Jones (2003), Computation of electromagnetic resonance in the Earth-ionosphere duct by using a full-wave and a simplified model (in Russian), *Radiophyz. Electron.*, *8*(1), 55–66.

Madden, T., and W. Thompson (1965), Low-frequency electromagnetic oscillations of the Earth-ionosphere cavity, *Rev. Geophys.*, *3*(2), 211–245.

Melnikov, A., A. P. Nickolaenko, G. Sátori, and C. Price (2002), Diurnal-seasonal variations in the Schumann resonance: Terminator effect or source-receiver distance effect?, paper presented at 2002 URSI General Assembly, Union Radio. Sci. Int., Maastricht, Netherlands.

Melnikov, A., C. Price, G. Sátori, and M. Fullekrug (2004), Influence of solar terminator passages on Schumann resonance parameters, *J. Atmos. Sol. Terr. Phys.*, *66*, 1187–1194.

Morente, J. A., G. J. Molina-Cuberos, J. A. Portí, B. P. Besser, A. Salinas, K. Schwingenschuch, and H. Lichtenegger (2003), A numerical simulation of Earth's electromagnetic cavity with the transmission line matrix method: Schumann resonances, *J. Geophys. Res.*, *108*(A5), 1195, doi:10.1029/2002JA009779.

Mushtak, V. C., and E. R. Williams (2002), ELF propagation parameters for uniform models of the Earth-ionosphere waveguide, *J. Atmos. Sol. Terr. Phys.*, *64*, 1989–2001.

Nickolaenko, A. P. (1986), ELF radio wave scattering by the global non-uniformities of the Earth-ionosphere cavity, *Izv. Vyssh. Uchebn. Zaved Radiophyz.*, *29*, 33–40.

Nickolaenko, A. P., and M. Hayakawa (2002), *Resonances in the Earth-Ionosphere Cavity*, Springer, New York.

Nickolaenko, A. P., and L. M. Rabinowicz (1974), Speeding up the convergence of the zonal harmonic series representation in the Schumann resonance problem, *J. Atmos. Terr. Phys.*, *36*, 979–987.

Nickolaenko, A. P., and L. M. Rabinowicz (1982), On the possibility of existence of global electromagnetic resonances on the planets of solar system, *Space Res.*, *20*, 82–89.

Nickolaenko, A. P., M. Hayakawa, and Y. Hobara (1996), Temporal variations of the global lightning activity deduced from the Schumann resonance data, *J. Atmos. Terr. Phys.*, *58*, 1699–1709.

Nickolaenko, A. P., O. Pechony, and C. Price (2006), Model variations of Schumann resonance based on Optical Transient Detector maps of global lightning activity, *J. Geophys. Res.*, *111*, D23102, doi:10.1029/2005JD006844.

Otsuyama, T., D. Sakuma, and M. Hayakawa (2003), FDTD analysis of ELF wave propagation and Schumann resonances for a subionospheric waveguide model, *Radio Sci.*, *38*(6), 1103, doi:10.1029/2002RS002752.

Pechony, O., and C. Price (2004), Schumann resonance parameters calculated with a partially uniform knee model on Earth, Venus, Mars, and Titan, *Radio Sci.*, *39*, RS5007, doi:10.1029/2004RS003056.

Pechony, O., and C. Price (2006), Schumann resonances: Interpretation of local diurnal intensity modulations, *Radio Sci.*, *41*, RS2S05, doi:10.1029/2006RS003455 [printed *42*(2), 2007].

Price, C. (2000), Evidence for a link between global lightning activity and upper tropospheric water vapor, *Nature*, *406*, 290–293.

Price, C., and M. Asfur (2007), Can lightning observations be used as an indicator of upper-tropospheric water-vapor variability?, *Bull. Am. Meteorol. Soc.*, *87*(3), 291–298, doi:10.1175/BAMS-87-3-291.

Rabinowicz, L. M. (1986), On the impact of the day-night nonuniformity of the LELF fields, *Izv. Vyssh. Uchebn. Zaved Radiophyz.*, *29*, 635–644.

Rabinowicz, L. M. (1988), Global electromagnetic resonances in non-uniform and anisotropic Earth-ionosphere cavity, Ph.D. thesis, Kharkov State Univ., Kharkov, Ukraine.

Sátori, G., M. Neska, E. Williams, and J. Szendrői (2007), Signatures of the day-night asymmetry of the Earth-ionosphere cavity in high time resolution Schumann resonance records, *Radio Sci.*, doi:10.1029/2006RS003483, in press.

Sentman, D. D. (1990), Electrical conductivity of Jupiter's shallow interior and the formation of a resonant planetary-ionosphere cavity, *Icarus*, *88*, 73–86.

Sentman, D. D., and B. J. Fraser (1991), Simultaneous observation of Schumann resonances in California and Australia: Evidence for intensity modulation by local height of the *D* region, *J. Geophys. Res.*, *96*, 15,973–15,984.

Schumann, W. O. (1952), On the radiation free self-oscillations of a conducting sphere which is surrounded by an air layer and an ionospheric shell, *Z. Naturforsch. A*, *7*, 149–154.

Wait, J. R. (1964), On the theory of Schumann resonances in the Earth-ionosphere cavity, *Can. J. Phys.*, *42*, 575–582.

Whipple, F. J. W. (1929), On the association of the diurnal variations of electric potential in fine weather with the distribution of thunderstorms over the globe, *Q. J. R. Meteorol. Soc.*, *55*, 1–17.

Williams, E. R. (1992), The Schumann resonance: A global tropical thermometer, *Science*, *256*, 1184–1186.

Williams, E. R., and G. Sátori (2004), Lightning, thermodynamic and hydrological comparison of the two tropical continental chimneys, *J. Atmos. Sol. Terr. Phys.*, *66*, 1213–1231.

Yang, H., and V. P. Pasko (2005), Three-dimensional finite difference time domain modeling of the Earth-ionosphere cavity resonances, *Geophys. Res. Lett.*, *32*, L03114, doi:10.1029/2004GL021343.

Yang, H., and V. P. Pasko (2006), Three-dimensional finite difference time domain modeling of the diurnal and seasonal variations in Schumann resonance parameters, *Radio Sci.*, *41*, RS2S14, doi:10.1029/2005RS003402 [printed *42*(2), 2007].

Yatsevich, E. I., A. P. Nickolaenko, A. V. Shvets, and L. M. Rabinowicz (2005), Two component source model of Schumann resonance signal, *Radiophiz. Elektron.*, *10*(2), 224–232.

A. P. Nickolaenko, Usikov Institute for Radio Physics and Electronics, Ukrainian National Academy of Sciences, Kharkov 61085, Ukraine. (sasha@ire.kharkov.ua)

O. Pechony and C. Price, Department of Geophysics and Planetary Sciences, Tel Aviv University, Tel Aviv 69978, Israel. (pechony@gmail.com; cprice@flash.tau.ac.il)